phloem cells is based entirely on the histology of extant materials (*13*). This study provides a basis for the continued examination of vascular plant phloem in the fossil record, and suggests that additional refinement of paleobotanical techniques may lead to a greater understanding of phloem evolution.

EDITH L. SMOOT
THOMAS N. TAYLOR
Department of Botany, Ohio State University, Columbus 43210

References and Notes

1. Features used to distinguish extant phloem cells include organelle composition and ultrastructure and staining properties of the protoplast. See Esau (*2*) for further information.
2. K. Esau, *The Phloem* (Borntraeger, Berlin, 1969).
3. E. L. Smoot and T. N. Taylor, *Am. J. Bot.* **65**, 571 (1978).
4. C. W. Good and T. N. Taylor, *Palaeontology* **13**, 29 (1970).
5. The use of the general term sieve element conforms to the terminology of Esau (*2*, p. 9) and designates the basic cell type of the phloem tissue, which is involved in conduction of organic solutes in plants. See also the discussions of phloem terminology in M. Kruatrachue and R. F. Evert [*Am. J. Bot.* **61**, 253 (1974)] and J. W. Perry and R. F. Evert [*ibid.* **62**, 1038 (1975)].
6. R. R. Dute and R. F. Evert, *Am. J. Bot.* **64**, 421 (1977); R. D. Warmbrodt and R. F. Evert, *ibid.* **61**, 267 (1974).
7. C. B. Beck, *ibid.* **44**, 350 (1957); J. Galtier and C. Hébant, *C. R. Acad. Sci. Ser. D* **267**, 2257 (1973); J. W. Hall, *Am. Midl. Nat.* **47**, 763 (1952); S. E. Scheckler and H. P. Banks, *Am. J. Bot.* **58**, 737 (1971); *ibid.*, p. 874; M. L. Wilson and D. A. Eggert, *Bot. Gaz. (Chicago)* **135**, 319 (1974).
8. D. A. Eggert and D. D. Gaunt, *Am. J. Bot.* **60**, 755 (1973).
9. D. A. Eggert and N. Y. Kanemoto, *Bot. Gaz. (Chicago)* **135**, 102 (1977).
10. D. F. Satterthwait and J. W. Schopf, *Am. J. Bot.* **59**, 373 (1972).
11. C. G. K. Ramanujam and W. N. Stewart, *ibid.* **56**, 101 (1969).
12. M. L. Wilson and D. A. Eggert, *Bot. Gaz. (Chicago)* **135**, 319 (1974).
13. K. Esau, V. I. Cheadle, E. F. Gifford, *Am. J. Bot.* **40**, 9 (1953).
14. Supported by NSF grants DEB77-02239 and DEB-01714.

12 June 1978; revised 16 August 1978

Rapid Light-Induced Changes in Near Infrared Transmission of Rods in *Bufo marinus*

Abstract. *Rapid transient changes in axial transmission of near infrared light through the outer segments of retinal rods of* Bufo marinus *are induced by illumination. The reasons for these changes are not clear. The changes in optical transmission may be useful in the study of photoreceptor function. However, the study of photoreceptor functions through the use of indicator dyes may be confounded by the intrinsic light-induced changes of optical properties of the photoreceptor cells.*

Retinal rods of *Bufo marinus* exhibit rapid light-induced changes in optical transmission for wavelengths longer than 650 nm; these transmission changes are too large to be attributed to changes in the absorption of rhodopsin or its photoproducts. This finding is surprising because the absorbance of rhodopsin (*1*) falls to below 0.1 percent of its peak value at wavelengths longer than 650 nm, and decreases approximately tenfold for each additional 30-nm increase in wavelength (*2*). Moreover, in the vertebrate retina, all known photoproducts that can be measured on the time scale of our experiments have absorbance maximums at wavelengths shorter than the parent rhodopsin and have no apparent secondary peaks at longer wavelengths. Therefore, the bleaching of rhodopsin or its photoproducts could account for no more than a 0.1 percent change in optical transmission through the rods at 650 nm and no more than a 10^{-6} percent change at 870 nm.

We mounted the isolated retina of *B. marinus* receptor-side up in a transparent dish on the stage of a compound microscope; oxygenated Ringer's solution (*3*) flowed through the dish. Both the stimulus beam (used to elicit photoreceptor responses) and the measuring beam (used to determine optical transmission) were directed at the retina through the microscope condenser (*4*).

The image of one, or many, of the rods whose axes were aligned with the optical axis of the microscope was focused on a photodetector (*5*) by means of a microscope objective (*6*). The wavelength of the measuring beam was selected by means of an interference filter (*7*) and was chosen to be in the far red or near infrared, away from the peaks of the absorption spectra of rhodopsin and its photoproducts. The measuring beam bleached an insignificant fraction of the rhodopsin, for example, no more than 5 rhodopsin molecules per rod per second for an 870-nm light (*8*). The stimulus light was restricted to wavelengths between 365 and 625 nm by an interference cutoff filter. For some experiments, single rod outer segments were impaled with micropipettes (*3*). In these experiments the measuring beam was passed through an interference filter (660 nm) and was also used as the stimulus; it bleached 6.4×10^4 rhodopsin molecules per rod per second.

A brief stimulus induced a change in optical transmission for a long-wavelength measuring light (Fig. 1). Changes in transmission were observed when measurements were made with light passing either through an area of retina that contained many hundreds of rods (Fig. 1) or through only a single rod (Fig. 2). The time course of these changes in transmission differed from that of the receptor potential (Fig. 2). The transmission changes had an action spectrum that was consistent with the absorption spectrum of rhodopsin (*9*); these changes disappeared after all the rhodopsin had been bleached (Fig. 1).

The rapid light-induced changes in transmission have the following properties. They fail to occur shortly after the flow of perfusate is stopped (*10*). They occur in retinas bathed in perfusate to which 2 m*M* aspartate has been added; therefore, they do not depend upon the activity of the proximal retinal neurons (*11*) and must arise in the rods. They persist in perfusate low in Na^+ (*3*); therefore, they do not depend on light-induced changes of ionic fluxes across the plasma membranes of the rods. A change in birefringence (*12*) does not account for the transmission changes because they were not attenuated after both the residual polarization of the incident light and the polarization sensitivity of the photodetector were reduced (*13*). Also, the transmission changes were not observed when the retina was placed between crossed polaroids (*14*). However, the amplitude of the transmission changes varied inversely with the numerical apertures of both the condenser and the objective.

The waveform of the transmission changes depended on stimulus irradiance and had a long duration that sometimes exceeded 10 seconds. The latency of the change in transmission was inversely related to stimulus irradiance. The lowest values of irradiance [with, for example, a 4.2 neutral density (ND) filter in Fig. 1] elicited a slow transmission increase, whereas higher values also elicited a more rapid component, a transmission decrease (3.0, 2.4, and 1.8 ND in Fig. 1). Thus, the higher values of irradiance elicited biphasic changes (for example, 3.0 and 1.8 ND in Fig. 1) or more complicated waveforms (for example, 2.4 ND in Fig. 1). The apparent drift of the baseline (Fig. 1) is probably attributable to stimulation by the measuring beam itself. The drift was more rapid for measurements at 750 nm than at 850 or 870 nm and was not seen after all the photopigment was bleached.

In three experiments, we measured changes in optical transmission at both 870 and 750 nm for the same retinal

0036-8075/78/1208-1083$00.50/0

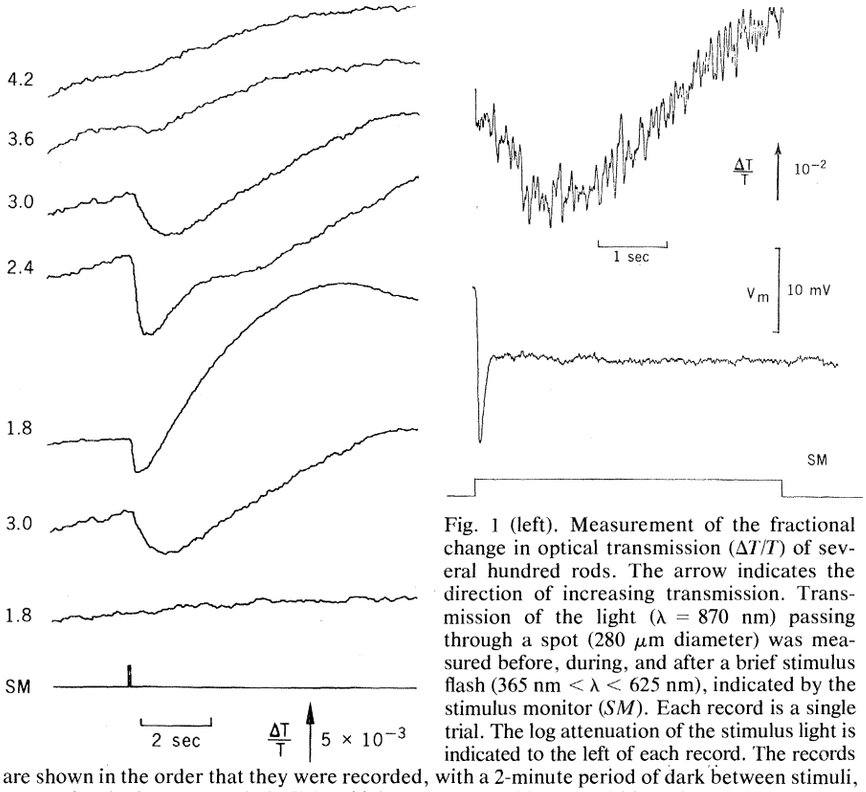

Fig. 1 (left). Measurement of the fractional change in optical transmission ($\Delta T/T$) of several hundred rods. The arrow indicates the direction of increasing transmission. Transmission of the light (λ = 870 nm) passing through a spot (280 μm diameter) was measured before, during, and after a brief stimulus flash (365 nm $< \lambda <$ 625 nm), indicated by the stimulus monitor (*SM*). Each record is a single trial. The log attenuation of the stimulus light is indicated to the left of each record. The records are shown in the order that they were recorded, with a 2-minute period of dark between stimuli, except for the last record (1.8 ND), which was preceded by a total bleaching of the photopigment in the retina. The irradiance of the measuring light was 1.2×10^{-2} W/cm^2. The irradiance of the unattenuated stimulus light was 1.5×10^{-3} W/cm^2. The numerical aperture of the microscope condenser and objective were 0.29 and 0.08, respectively. Fig. 2 (right). Simultaneous measurements of the fractional change in optical transmission ($\Delta T/T$) and membrane potential (V_m) from two different rods in the same retina. Transmission of the light that emerged from a single rod outer segment was measured while membrane potential was recorded with a pipette placed in a neighboring outer segment. A single light (λ = 660 nm) was used to stimulate the retina and measure transmission; the time course of this light is indicated by tracing *SM*; the irradiance was 2.8×10^{-4} W/cm^2. The numerical apertures of the microscope condenser and objective were 0.10 and 0.20, respectively.

areas. For both wavelengths, the measuring beams had irradiances of approximately 1.5×10^{-2} W/cm^2. For bright stimuli (365 nm $< \lambda <$ 625 nm; irradiance $\geq 10^{-5}$ W/cm^2) the transmission changes at both wavelengths were similar in amplitudes and waveforms. For dimmer stimuli, the transmission changes at 750 nm were difficult to detect in single sweeps because the measuring light itself apparently elicited changes of optical transmission. The waveform and sign of the light-elicited changes in transmission also depended on the numerical apertures of the condenser and objective as well as on the distance between the rod outer segments and the plane of focus of the objective.

Light-induced changes in optical transmission through isolated, disoriented rod outer segments have been reported (*15*); these changes in optical properties of outer segments may share a common mechanism with the changes in optical transmission that we report. They may arise from either a change in light scattering by the rod outer segments or a change in the distribution of light reflected internally within the outer segments, or both (*16*). Since these transmission changes occur rapidly, they may supplement the receptor potential as a useful measure of the physiology of the rod outer segment. Since these changes occur in unstained retinas, they will have to be taken into account in any study of photoreceptor or retinal function that monitors absorption changes, including those studies employing metallochromic indicator dyes (*17*), *p*H indicator dyes, or voltage-sensitive dyes (*18*).

H. H. HARARY
Committee on Higher Degrees in Biophysics, Harvard University, Cambridge, Massachusetts 02138
J. E. BROWN
Department of Physiology and Biophysics, State University of New York, Stony Brook 11794
L. H. PINTO
Department of Biological Sciences, Purdue University, West Lafayette, Indiana 47907

References and Notes

1. The absorbance spectrum of rhodopsin in solution and in living retinas approximates the spectral sensitivity of retinal rods, and both absorbance and spectral sensitivity are low at wavelengths longer than 650 nm. The absorbance of rhodopsin in the far red is so low that the most reliable estimates available are based on measurement of spectral sensitivity [S. Hecht, *Am. Sci.* **32**, 159 (1944); G. Wald, *Science* **101**, 653 (1945); F. Crescitelli and H. J. A. Dartnall, *Nature (London)* **172**, 195 (1953); R. Granit, *Receptors and Sensory Perception* (Yale Univ. Press, New Haven, 1955), p. 114; G. Wald and P. K. Brown, *Science* **127**, 222 (1958); G. Wald, P. K. Brown, I. R. Gibbons, *J. Opt. Soc. Am.* **53**, 20 (1963); A. Knowles and H. J. A. Dartnall, in *The Eye*, vol. 2, part B, *The Photobiology of Vision*, H. Davson, Ed. (Academic Press, New York, 1960), pp. 458-460].
2. D. R. Griffin, R. Hubbard, G. Wald, *J. Opt. Soc. Am.* **37**, 546 (1947).
3. J. E. Brown and L. H. Pinto, *J. Physiol. (London)* **237**, 575 (1974); J. E. Brown, J. A. Coles, L. H. Pinto. *ibid.* **269**, 707 (1977).
4. The numerical aperture of the condenser could be varied from <0.1 to 0.6.
5. The photodetector was either a silicon photodiode (PV 100, E G & G, Salem, Mass.) or a photomultiplier tube (Hamamatsu R777, Middlesex, N.J.). A pinhole or an iris diaphragm was placed in the image plane of the objective to restrict the light reaching the photodetector to that light passing through either a single photoreceptor or many photoreceptors.
6. For the electrophysiological experiments and the measurements on single rods, a water-immersion objective (×40) with a variable numerical aperture (<0.05 to 0.75) was used. For measurements from larger areas of the retina (Fig. 1) a 20-power objective, with variable numerical aperture (<0.05 to 0.20) was used; in this case a cover glass was used to cover the dish so that the measuring beam did not cross an air-water interface.
7. Interference filters had center wavelengths of 660, 750, 850, and 870 nm with the bandwidth at half maximum transmission of 10 nm. The 750-, 850-, and 870-nm filters were blocked sufficiently to short wavelengths that the unattenuated stimulus (365 $< \lambda <$ 625 nm) was not detected by the photodetector.
8. The rate at which rhodopsin molecules were bleached was calculated as follows. The irradiance in the plane of the outer segments was 1.2×10^{-2} W/cm^2 at λ = 870 nm (measured with a J16 photometer, Tektronix, Beaverton, Ore.). Assuming that the cross-sectional area of a rod is 44 μm^2, the quantum efficiency is 0.5 and the photosensitivity at 870 nm is 9.4 orders of magnitude less than the photosensitivity at the peak of the rhodopsin absorbance spectrum (*2*), the measured irradiance would result in the bleaching of 5 rhodopsin per rod per second.
9. The area of retina that contained several hundred rods also contained an unknown number of cones. It is unlikely that the transmission changes recorded can be attributed to these cones, both because the signals could be recorded from single rods and because the action spectrum of the changes matched the absorbance spectrum of rhodopsin.
10. Stopping the flow of perfusate caused the retinal function to deteriorate; that is, either receptor potentials became smaller and slower or the rod outer segments became structurally distorted, or both.
11. L. Cervetto and E. F. MacNichol, Jr., *Science* **178**, 767 (1972).
12. P. A. Liebman, W. S. Jagger, M. W. Kaplan, F. G. Bargoot, *Nature (London)* **251**, 31 (1974).
13. The residual plane polarization of the incident light beam was reduced from 20 percent to less than 0.1 percent by placing a "wedge depolarizer" (Burleigh Optics, Burleigh, N.J.) either above or below the microscope condenser. The plane polarization sensitivity of the photomultiplier was reduced to less than 0.5 percent by placing a quarter-wave retardation plate in front of the photomultiplier.
14. Polaroid material (HN22, Polaroid, Cambridge, Mass.) was used because of its high extinction ratio in the far red.
15. K. P. Hofmann, R. Uhl, W. Hoffmann, W. Kreutz, *Biophys. Struct. Mech.* **2**, 61 (1976); R. Uhl, K. P. Hofmann, W. Kreutz, *Biochim. Biophys. Acta* **469**, 113 (1977); C. L. Wey and R. A. Cone, *Biophys. J.* **21**, 135a (1978).
16. It is possible that the changes in optical transmission might occur in the inner segment of an intact rod; if this were true, then excitation of the activated rhodopsin molecules would have

to be communicated from the outer to the inner segment in the absence of both changes of membrane voltage and current flow between outer and inner segments (in perfusate low in Na^+). Such intracellular transmission of excitation might be accomplished by diffusion of an intracellular messenger substance. However, because light-induced changes of optical transmission have been observed from isolated rod outer segments, we think that the changes in transmission measured from intact rods occur in the outer segments.
17. For examples, arsenazo III: J. E. Brown, L. B. Cohen, P. DeWeer, L. H. Pinto, W. N. Ross, B. M. Salzberg, *Biophys. J.* **13**, 1155 (1975); J. E. Brown, P. K. Brown, L. H. Pinto, *J. Physiol. (London)* **267**, 299 (1977).
18. W. N. Ross, B. M. Salzberg, L. B. Cohen, A. Grinvald, H. Davila, A. Waggoner, C. Wang, *J. Membr. Biol.* **33**, 141 (1977).
19. We wish to thank J. E. Dowling for his support and encouragement. We thank P. K. Brown, F. D. Carlson, T. G. Goldsmith, R. Hubbard, D. H. Kelley, and H. Ripps for their thoughtful comments on the manuscript. Supported by NIH training grant 5701 GM00782-19 (to H.H.H.), NIH grants EY 01914 and EY 01915 (to J.E.B.), and EY 01221 (to L.H.P.).

24 February 1978; revised 6 July 1978

Mediterranean Water: An Intense Mesoscale Eddy off the Bahamas

Abstract. *An anticyclonic lens of water in the permanent thermocline off the Bahamas has water mass characteristics representing Mediterranean and eastern Atlantic central waters. This eddy's ability to translate across the Atlantic without losing its identity points to baroclinic eddies as a specific mechanism for large-scale mixing.*

Thermocline waters of the North Atlantic are characterized by an extremely tight relationship between temperature (T) and salinity (S) in the range from 6° to 17°C. Geographical variations in this T/S relationship are caused mainly by intrusions of relatively saline Mediterranean water and fresher Antarctic intermediate water. The hydrographic treatise of Iselin (*1*) and the more recent volumetric census of Wright and Worthington (*2*) suggest that T/S anomalies in the western North Atlantic imposed by these two water masses are limited to temperatures less than 8°C. Recent hydrographic observations from the western Sargasso Sea revealed an anomalously saline water mass ranging from 7° to 12°C which was embedded in the thermocline. The characteristics of this feature indicate that it contained water from the eastern Atlantic and the Mediterranean Sea. This report is a presentation of the property anomalies associated with this intense baroclinic eddy.

The mass of highly saline thermocline water was discovered in the Hatteras abyssal plain during cruise 15 of the R.V. *Oceanus* in October 1976. This Mediterranean eddy (or "Meddy") was initially detected during a survey in which 750-m expendable bathythermograph probes (XBT's) were dropped in a 1° square centered at 25°N, 70°W. The Meddy appeared as an extremely warm feature in the temperature field below 700 m, with resulting horizontal temperature gradients as large as 1°C in 30 km. Although the XBT-derived temperature-depth measurements did not penetrate the lower limit of the lens, the nearly circular geometry and 100-km radius were evident.

After the XBT survey, a series of 32 lowerings of a salinity-temperature-depth (STD) recorder were made within 150 km of the Meddy. Continuous vertical profiles were obtained from the surface to a depth of 1500 m at each station. Figure 1 is a composite of nine T/S curves obtained at various radial distances from the center of the Meddy. These profiles illustrate the rich vertical structure of both temperature and salinity within the Meddy. Temperatures within the Meddy exceeded those of surrounding stations in the depth range from 700 to 1300 m; for example, 10°C water was observed at 1010 m inside the Meddy and generally remained near 800 m for all far-field stations. The vertical temperature gradient within the Meddy was also highly depth-dependent: at 900 and 1100 m the gradients were 0.7°C/100 m and 2.8°C/100 m, respectively, compared to typical values of 2.0°C/100 m. Although vertical temperature profiles were smooth and monotonically decreasing with depth at stations taken outside the Meddy, significant temperature inversions were evident in profiles taken around its periphery. The largest of these inversions extended between 970 and 1020 m at a station approximately 35 km from the center of the Meddy.

The distribution of salinity in the vicinity of the Meddy was similar to the general characteristics of the temperature field. Salinities within the Meddy ex-

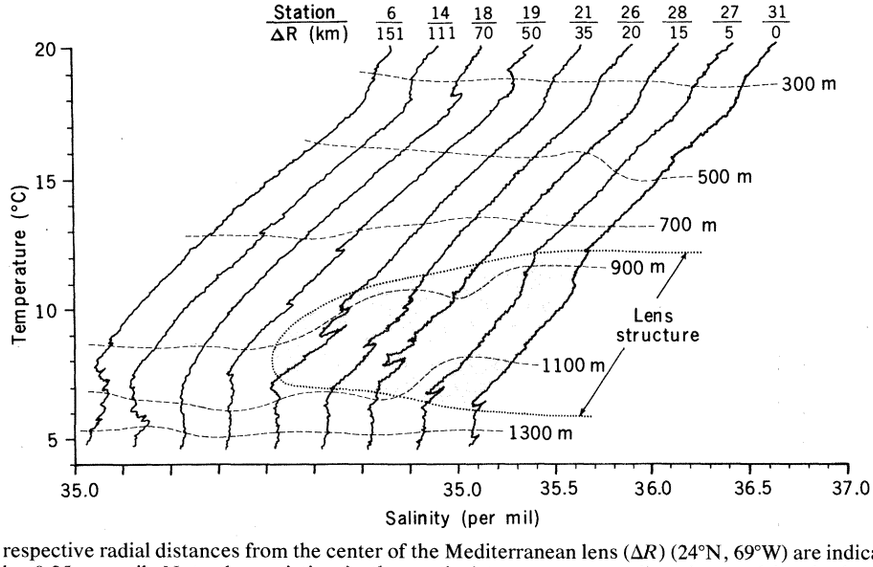

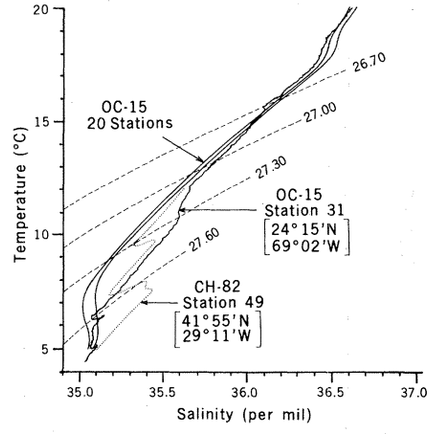

Fig. 1 (left). Temperature/salinity curves through the main thermocline for selected stations occupied during R.V. *Oceanus* cruise 15, October 1976. Station numbers and their respective radial distances from the center of the Mediterranean lens (ΔR) (24°N, 69°W) are indicated. Each successive profile has been displaced by 0.25 per mil. Note the variation in the vertical temperature gradient imposed by the lens. Portions of individual curves which contain excessively high salinities are shaded to illustrate the temperature range and the horizontal and vertical scales of this feature. Fig. 2 (right). Temperature/salinity curves from R.V. *Oceanus* cruise 15, station 31, within the lens of Mediterranean water, and R.V. *Chain* cruise 82, station 49, at the Mid-Atlantic Ridge (*5*). An envelope enclosing 1 standard deviation from the mean T/S curve of 20 *Oceanus* cruise 15 stations outside the lens illustrates the typical characteristics of thermocline waters in the survey region. Dashed lines are σ_t curves.

0036-8075/78/1208-1085$00.50/0